Letters on Materials 12 (3), 2022 pp. 243-248 www.lettersonmaterials.com

https://doi.org/10.22226/2410-3535-2022-3-243-248

Check for updates

Computer and physical modeling of multiple isothermal forging of EK61 superalloy

E. V. Galieva†, A. Kh. Akhunova, V. A. Valitov, E. Yu. Klassman

†galieva_elvina_v@mail.ru

Institute for Metals Superplasticity Problems, RAS (IMSP RAS), Ufa, 450001, Russia

Studies on the process of multiple isothermal forging of high-temperature nickel-based EK61 superalloy using computer simulation in the DEFORM-3D software package in a three-dimensional formulation and a comparison with experimental data were carried out. Based on the simulation results, it is shown that with each subsequent stage of forging, the maximum strain values become higher, and the strain differences in the central and peripheral regions become smaller. Such a strain distribution leads to the formation of a homogeneous ultrafine-grained (UFG) microstructure. The initial coarse-grained microstructure is gradually transformed into a fine-grained microduplex type microstructure at $0.77T_{melt}$ and with a further decrease in the processing temperature to $0.73T_{melt}$, it is transformed into a submicroduplex type (γ + δ) UFG microstructure.

Keywords: multiple isothermal forging, ultrafine-grained microstructure, computer modeling, experimental modeling, Ni-based superalloy.

1. Introduction

Heat-resistant nickel-based superalloys belong to a unique class of materials capable of operating at elevated temperatures and in corrosion environment due to their complex chemical composition. Therefore, superalloys are widely used for the manufacture of various parts for aircraft gas turbine engines, as well as for rocket engines [1–12]. The complex chemical composition of modern superalloys provides the required characteristics of the heat-resistant property due to solid solution hardening and the precipitation of the strengthening coherent phases. But it also leads to a significant decrease in the technological plasticity and increase in labor intensity during processing. It is known [4 – 6] that the most efficient method to increase the technological plasticity of superalloys is the formation of an UFG microstructure in bulk semi-finished products. Such a microstructure is necessary for realizing the structural superplasticity effect in technological processes of manufacturing of various articles, for example, gas turbine engine parts. Deformation-heat treatment (DHT) is traditionally used to form the duplex type UFG microstructure in hard-to-deform superalloys [4 – 8]. To obtain a micro-duplex microstructure in the superalloys strengthened by Ni_3(Al, Ti) intermetallic phases, the DHT is mainly used in the two-phase γ+γ'-region by means of uniaxial compression [4, 5, 7].

A universal methodological approach to obtain UFG and nanocrystalline microstructures in bulk and sheet semi-finished products from nickel-based superalloys has been developed at IMSP RAS [4, 5, 7,13 –16]. This method consists in carrying out DHT using a scheme of multiple isothermal forging (MIF) with a step-by-step decrease of temperature from $(0.9…0.8)T_{melt}$ to $(0.6…0.5)T_{melt}$ in the processing [7,13 –18]. Such processing results in a stage-by-stage microstructure refinement: the coarse-grained microstructure is transformed into a fine-grained duplex type microstructure, then at a lower processing temperature (second stage) it is transformed into an UFG microstructure with a grain size reduced to the values below 1 μm. Thus, the microstructure refinement can be achieved down to the sizes in the range of nanometers. Formation of the UFG microstructure makes it possible to achieve the low-temperature superplasticity effect at temperatures (200…300)°C lower as compared to the one of traditional high-temperature superplasticity, which is observed in superalloys with a fine-grained duplex type microstructure [7,17,18].

Wrought EK61 superalloy is a representative of heat-resistant superalloys hardened by the γ''-phase [19 – 21]. In terms of chemical and phase compositions, this superalloy is the closest analogue to the well-known Inconel 718, which belongs to iron-nickel superalloys due to the high iron content [2]. Both EK61 and Inconel 718 superalloys contain more than 50% of nickel. The EK61 is used for the manufacture of large-sized stamped and welded structures of power installations operated at the temperature range from –253 to 750°C [19 – 21]. The γ''-phase precipitates after aging of both EK61 and the Inconel, but it is metastable and transforms into the thermally stable δ-phase during long-term aging or deformational heat treatment. Recent works [9, 22 – 24] were devoted to a study of the process of stamping and forging of superalloys under isothermal conditions at elevated temperatures by simulations, which make it possible to carry out a comprehensive comparative analysis of the deformation behavior and the stress-strain state and their interconnection

with microstructure change in forging during the stamping process. Nevertheless, the literature data on the simulation of isothermal forging are limited.

The purpose of this work is to study the stress-strain state and formation of homogeneous UFG microstructure in the MIF process of a wrought nickel EK61 superalloy by computer and experimental modeling.

2. Materials and Experimental Methods

In the initial state, the heat-resistant nickel EK61 superalloy was a hot-deformed rod with a diameter of 80 mm and initial coarse-grained microstructure (Fig. 1). As follows from the results of electron microscopic analysis (Fig. 1b), coherent nanosized ($d \approx 40$ nm) strengthening metastable γ''-phase (Ni_3Nb) particles are homogeneously distributed inside large grains of the γ-phase having an average size of about 62 μm. The chemical composition of EK61 is 58Ni-16.6Cr-15 Fe-3.9Mo-5Nb-Al-Ti-Cu-V [19, 25].

2.1. Experimental technique

To obtain an UFG microstructure in the EK61 superalloy, the DHT was carried out using the MIF scheme presented in [16]. A cylindrical billet with a diameter and a height of 80 mm was subjected to MIF which was carried out on a hydraulic press equipped with an isothermal stamp block (the force capability of 6.3 MN). Such processing was performed at the conditions established earlier in the temperature range of 950 – 850°C with a step-by-step decreasing of the temperature [25, 26]. At least 5-time pressings were performed at each temperature with a sequential rotation of the strain axis to 90°. The strain rate was $\dot{\varepsilon} \approx 10^{-2} - 10^{-3}$ s^{-1}. The total compression strain for forged billet was $e \approx 8$. The turning was performed to a workpiece size of $(40 \pm 2) \times (40 \pm 2) \times (250 \pm 5)$ mm^3 at the final step of the MIF. As noted above, EK61 is strengthened by intermetallic Ni_3Nb phases. Such phases have two modifications: low-temperature (γ''-phase, body-centered tetragonal ordered lattice (DO22)) and high-temperature (δ-phase plates with an orthorhombic lattice). The δ-phase is formed during aging or DHT in the temperature range of 650 – 980°C [2].

The microstructure of the superalloy was studied using an optical Carl Zeiss microscope, JEM-2000EX transmission electron microscope and Tescan Mira 3 LMH scanning electron microscope. The average grain size was determined by the secant method.

2.2. Computer simulation technique

Computer simulation of MIF was carried out in a three-dimensional formulation using the DEFORM-3D software package. A cylindrical sample with a diameter and height of 80 mm was subjected to MIF. The deforming tool (stamp) had the absolutely rigid body properties, the deformable body (sample) was assumed to an elastic-plastic one. The EK61 superalloy was considered as the workpiece material given by experimental curves obtained during uniaxial compression at the temperature of the forging. The finite elements number in the volume of the workpiece was 16 000. The contact conditions were described by the Siebel friction model. The value of the friction coefficient was taken equal to 0.3.

One of the important conditions for the effectiveness of the severe plastic strain method is the strain nonmonotonicity. In this regard, three steps of sample treatment were carried out at an initial strain rate of 10^{-3} s^{-1}. The temperature at each stage was decreased: 950°C (step 1), 900°C (step 2) and 850°C (step 3). Five-time pressing operations were performed when changing the axis of force application at each step:

step 1: pressing (compression strain ε = 50%) → turning by 90° and pressing (ε = 50%) → turning by 90° and pressing (ε = 48%) → turning by 45° and pressing (ε = 39%) → turning by 45° and pressing (ε = 38%);

step 2: pressing (compression strain ε = 50%) → turning by 90° and pressing (ε = 50%) → turning by 90° and pressing (ε = 35%) → turning by 45° and pressing (ε = 45%) → turning by 45° and pressing (ε = 44%);

step 3: pressing (compression strain ε = 50%) → turning by 90° and pressing (ε = 30%) → turning by 90° and pressing (ε = 23%).

The values of the accumulated strain were recorded after each transition at points on the same cross-sectional plane initially passing through the middle of the cylindrical sample

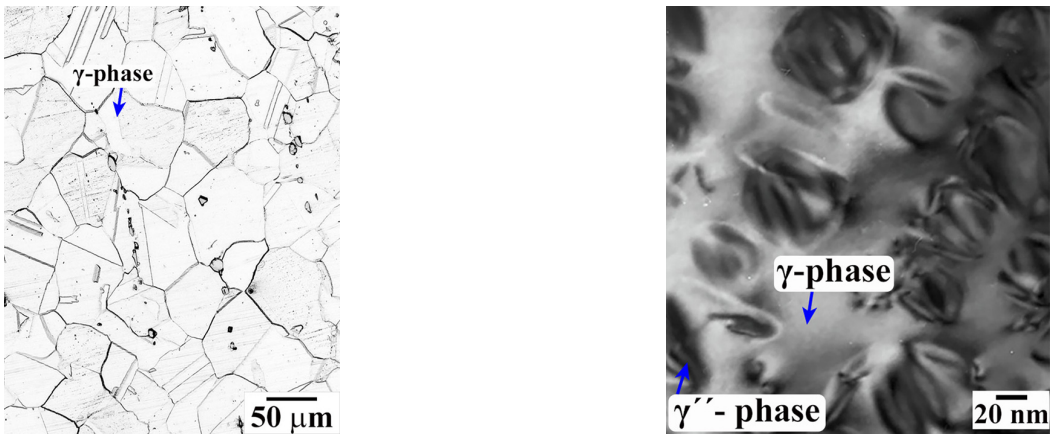

a b

Fig. 1. The initial coarse-grained microstructure of the EK61 superalloy studied by optical (a) and transmission electron microscopy (b).

obtained after the first transition at the first step. The initial position of this plane and the location of the control points are shown in Fig. 2. The following control points were considered: in the axial zone in the center of the sample (point 1) and near the end (point 2) close to the stagnant zone; and at half of the radius (points 3 – 5) equidistant from the center.

3. Results and discussion

Figure 3 shows the dependences of the values of accumulated strain taken at the control points on the transition number at all stages.

The accumulated strain in the sample increases with an increase in the number of transitions. The greatest value is observed in the sample center. The total accumulated values of the strain for points 1, 2 and 3 are the closest. The smallest value is observed for point 5. The diagrams of the distribution of equivalent strains at three steps are presented in Figs. 4 – 6.

Step 1. The strain in the center of the sample is higher than in the periphery at the first, second and fourth transitions (Fig. 4). The opposite picture is observed in the third and fifth transitions: the minimum values of the strain prevail in the center, while in the fifth transition a distinct deformation cross is formed, which indicates the shear nature of the strain. Thus, the central volume of the material is worked out more at the first, second and fourth transitions, the areas of the sample closer to the surface are worked out at the third and fifth transitions. In [9], simulations of isothermal forging of a nickel-base superalloy Waspaloy were carried out. A comparison of the strain distributions in the cited work and the results obtained for the first transition of step 1 of MIF (Fig. 4, transition 1) shows that they are similar. It is shown that the dead metal zones close to the dies are observed which is typical for a uniaxial compression scheme. Such inhomogeneous strain resulted in inhomogeneous formation of the microstructure [9].

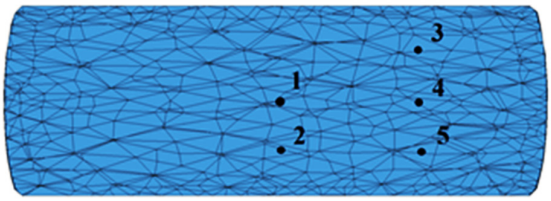

Fig. 2. Control points for determining the accumulated strain amount on the cross section of the sample obtained after the first transition of the MIF the at the first step.

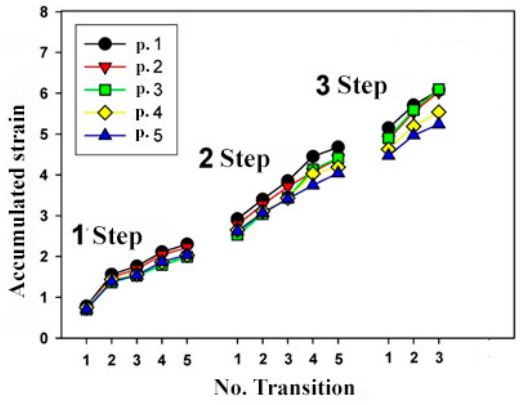

Fig. 3. (Color online) Dependence of the accumulated strain values at the control points in different steps and transitions of the MIF process.

Step 2 (Fig. 6). The maximum values of the strain prevail in the center in all transitions, except for the third one. The value of the strain in the center is less and increases as one proceeds further to the surface of the sample in the third transition. Therefore, those areas that were weakly deformed in previous transitions begin to be worked out.

Step 3 (Fig. 7). The minimum strain values are observed in the sample center at all transitions in contrast to the second one. The strain values increase as one proceeds further

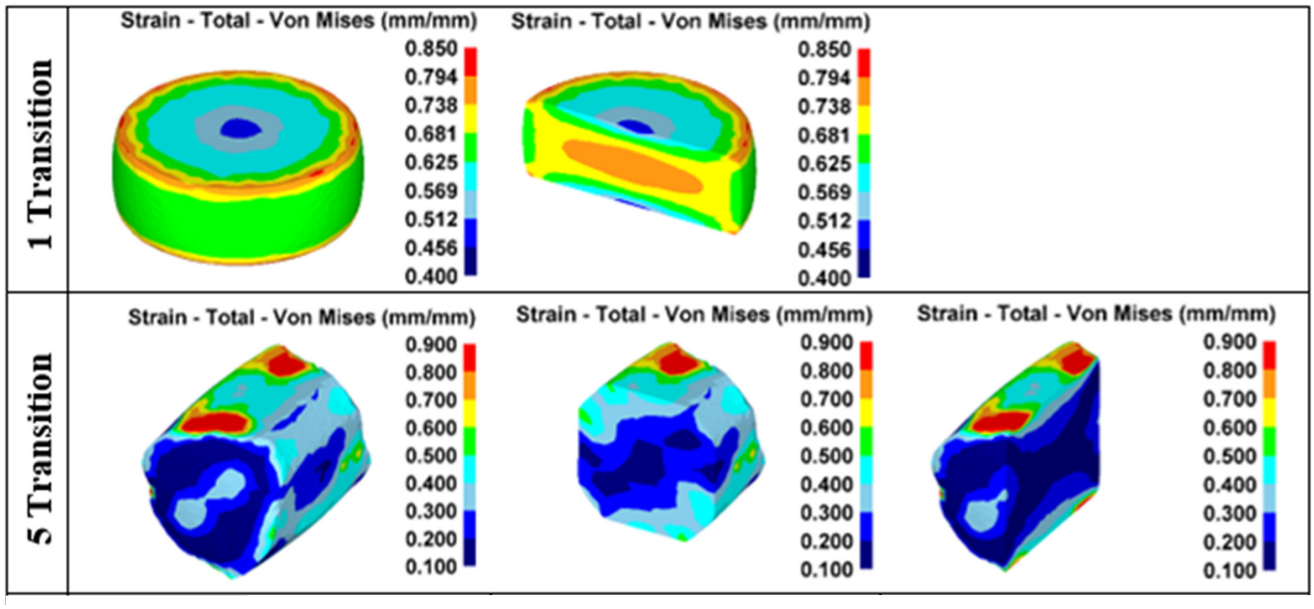

a b c

Fig. 4. (Color online) Diagrams of the distribution of equivalent strains in the sample at the first step (950°C) of the MIF. Sample shown in general view (a) and two perpendicular sections (b, c).

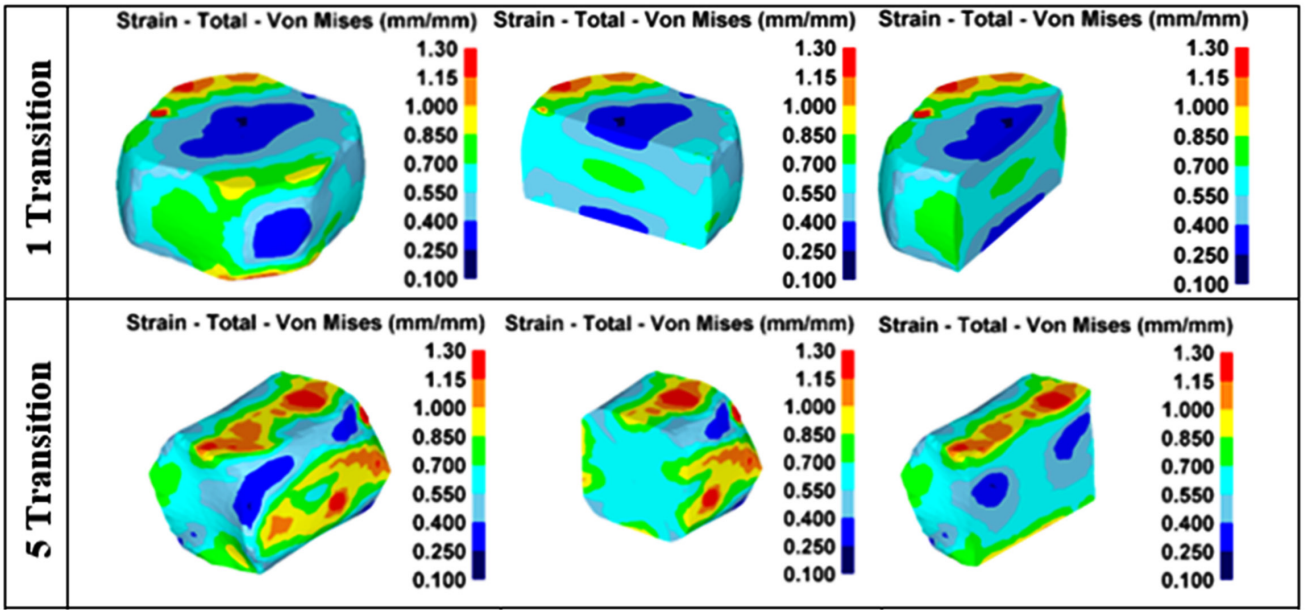

a b c

Fig. 5. (Color online) Diagrams of the distribution of equivalent strains in the sample at the second step (900°C) of the MIF. Sample shown in general view (a) and two perpendicular sections (b, c).

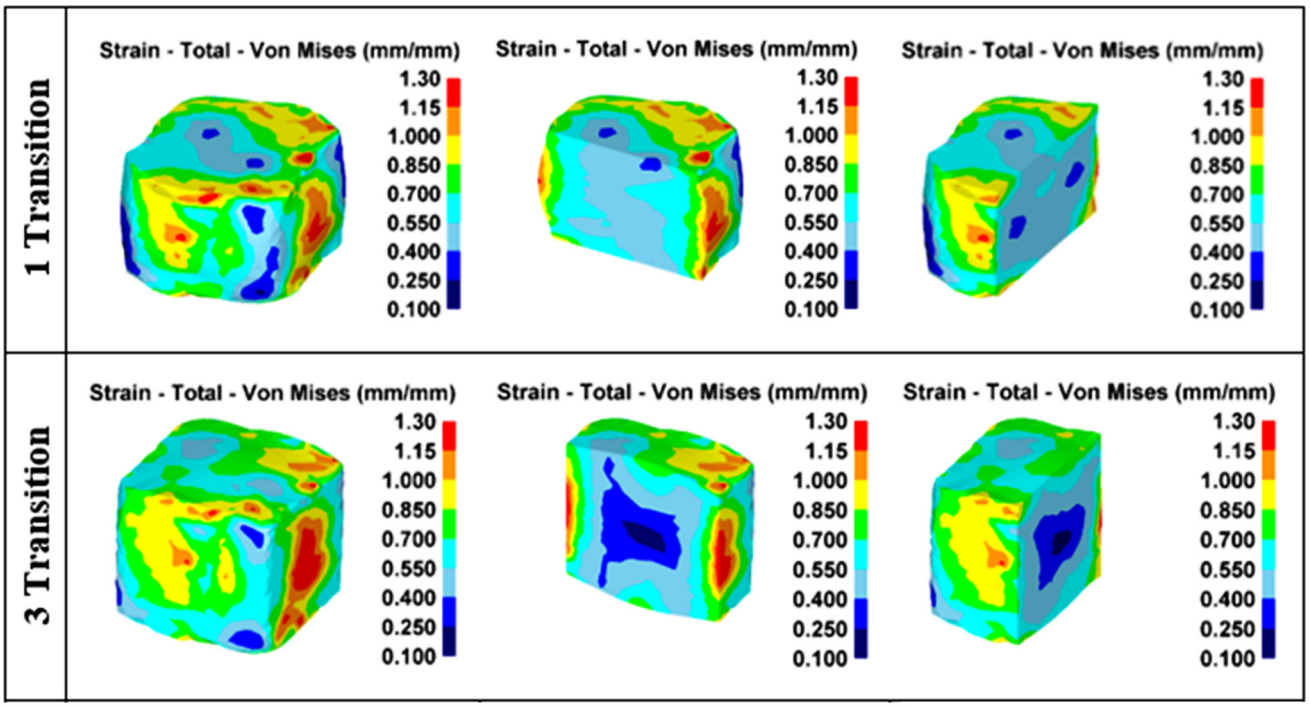

a b c

Fig. 6. (Color online) Diagrams of the distribution of equivalent strains in the sample at the third step (850°C) of the MIF. Sample shown in general view (a) and two perpendicular sections (b, c).

towards the periphery, while the strain distribution becomes more uniform than in the second stage.

Thus, the sample center is mainly worked out at the second step, while the periphery at the third one. Figures S1–S3 (Supplementary material) present the results of computer simulation of MIF in steps 1–3 at the transitions 1–5 in more details.

Figure 7a shows the microstructure of the EK61 after the second MIF step at 900°C. The results of the study showed that the initial coarse-grained microstructure was transformed into a duplex-type UFG one and new recrystallized equiaxed grains of the γ-phase free from dislocations were formed. The microstructure contains grains both with sizes less than 1 μm and about 1.8 μm. The high deformation temperature resulted in the transformation of the γ''-phase having a body-centered tetragonal lattice to the δ-phase having an orthorhombic lattice precipitated in the plate form. Microstructural analysis showed (Fig. 7b, c) that after the final step of the forging at

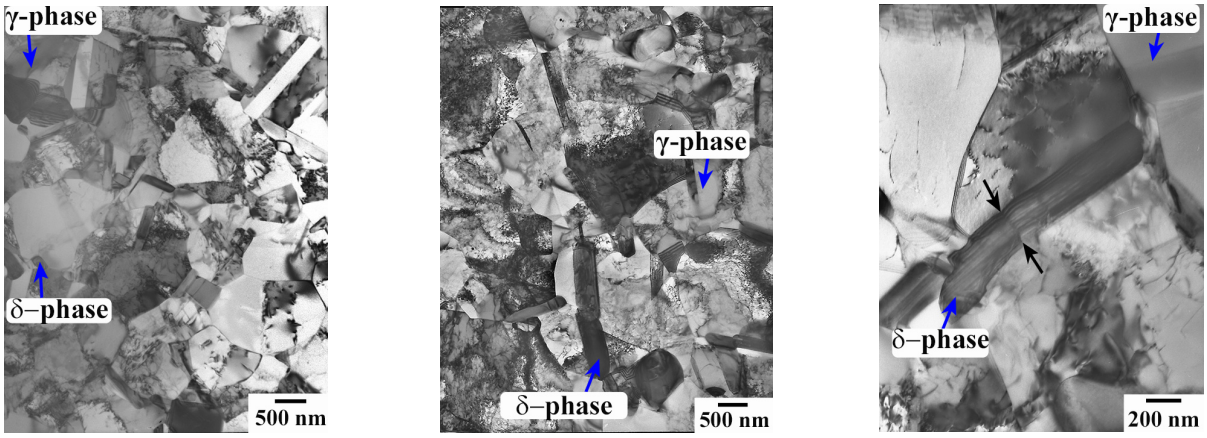

a b c

Fig. 7. Microstructure of the EK61 superalloy after MIF at the second step at a temperature of 900°C (a) and third step at a temperature of 850°C (b, c).

a low temperature of 850°C homogeneous UFG duplex-type microstructure was formed.

The average grain size of the γ-phase is 0.8 μm, the grain size of the δ-phase in the longitudinal direction is 0.75 μm and in the transverse one 0.2 μm. At the same time, there are individual large particles of the δ-phase up to 2 ± 0.5 μm in size, which are preserved and are "hereditary", formed at second stage of processing (Fig. S4).

Many intergranular and interfacial γ/δ boundaries exhibit a banded contrast of equilibrium high-angle boundaries (Fig. 7b). The segregations that have a globular incoherent ellipsoid shape of the thermally stable δ-phase are present mainly along the boundaries and in triple junctions of γ-phase grains. The largest particles of δ-phase of the lamellar form are divided (Fig. 7c, indicated by black arrows). It indicates processes of the δ-phase plate fragmentation during DHT and subsequent fragment spheroidization, which are transformed into incoherent particles that have smaller ellipsoidal shape. Comparative analysis of computer and experimental modeling data with the data presented in [18, 27, 28] after forging of Inconel 718 showed that the mechanism of formation of the submicroduplex type UFG microstructure in the EK61 superalloy during DHT is similar to the one was observed in Inconel 718. It is shown that the kinetics of the precipitation of the metastable strengthening γ''-phase and its thermally stable modification δ-phases have a significant effect on the behavior of the deformation and the nature of microstructural changes. An incubation period (at least 10 minutes) for the phase precipitation allows the MIF process to be carried out during some time. That is, it was possible to carry out strain with turning (at least 1 step, including 5 transitions) of the workpiece without cracking, since there was no additional precipitation, especially near the side surface of the workpiece, which is cooled and subjected to tensile stresses. It should be noted that when choosing conditions of MIF for superalloys characterized by low thermal conductivity, it is necessary to take account for the possibility of deformation heating of the workpiece. As shown in [29], even a uniaxial compression for one transition can lead to heating of the workpiece central zone. Such heating resulted in the dissolution of the strengthening γ'-phase and formation of the coarse-grained (40 μm) microstructure in the central zone of the workpiece. The author of the cited work showed that it was possible to minimize deformation heating in the case of workpiece fractional strain with strain degrees no more than 30 – 50%.

The computer and experimental modeling results of the MIF of the EK61 showed that significant strain occurs in the central zone. It can lead to strain heating in the central zone of the workpiece up to the dissolution temperature of the γ''-phase (or δ-phase). To minimize the negative effect of the deformation heating during high-temperature processing one can reduce the strain rate, for example, from 10^{-2} to 10^{-3} s^{-1}, as well as gradually decrease the processing temperature from 950 to 850°C. Based on the computer modeling results of the multiple isothermal forging process of the wrought EK61 superalloy, it was shown that in most transitions the maximum stresses are observed in the center of the sample, which reduces the probability of destruction of the sample surface. This is confirmed by the experimental results. It was established that wrought EK61 superalloy could be satisfactorily forged and no cracks were observed on the sample surface. At the same time, it was found that differences in strain distribution in billet becomes step by step smaller. The initial coarse-grained microstructure was transformed into a mixed ultrafine-grained microstructure duplex type. An average grain size of the γ-phase and incoherent particles of the δ-phase are less than 1 μm, as well as there are separate large particles of the δ-phase up to 2 ± 0.5 μm in size.

4. Conclusions

Based on the computer modeling and experimental results of the multiple isothermal forging process, it is shown that in each subsequent step of forging the differences in the values of the strain in the central and peripheral regions become smaller. Such distribution of the strain leads to the formation of a homogeneous submicroduplex type ultrafine-grained microstructure. New equiaxed recrystallized γ-phase grains free from dislocations are present. Thus, it is shown that multiple isothermal forging is an efficient method for obtaining a homogeneous UFG microstructure in billets of heat-resistant nickel superalloy of the EK61 type.

Supplementary material. *The online version of this paper contains supplementary material available free of charge at the journal's Web site (lettersonmaterials.com).*

Acknowledgement. The study in the part of computer modeling and development of the conditions for the formation of UFG microstructure in EK61 was supported by IMSP RAS state assignment No. 122011900470-7. The experimental part and detailed analysis of the UFG microstructure of the EK61 was financially supported by the Council on Grants of the President of the Russian Federation (Russian Federation President Scholarship No. SP-4002.2022.1). Electron microscopic studies were carried out on the shared services center facilities of IMSP RAS "Structural and Physical-Mechanical Studies of Materials".

References

1. Ch. Sims. Heat resistant materials for aerospace and industrial power plants. Moscow, Metallurgy (1995) 568 p. (in Russian)
2. R.C. Reed. The superalloys: Fundamentals and Applications. Cambridge University Press (2006) 372 p. Crossref
3. A.V. Logunov. Heat-resistant nickel alloys for blades and disks of gas turbines. Moscow, LLC Publishing House "Izdatel'skiy dom Gazoturbinnyye tekhnologii" (2017) 854 p. (in Russian)
4. O.A. Kaibyshev. Superplastisity, structure refinement and processing of hard-to-deform alloys. Moscow, Nauka (2002) 438 p. (in Russian)
5. R.R. Mulyukov, R.M. Imayev, A.A. Nazarov et al. Superplasticity of ultrafine-grained alloys: Experiment, theory, technologies. Moscow, Nauka (2014) 284 p. (in Russian)
6. B.S. Lomberg, S.V. Ovsepyan, M.M. Bakgradze, M.N. Letnikov, I.S. Mazlov. Aviation materials. S, 116 (2017). (in Russian) Crossref
7. V.A. Valitov. Letters on Materials. 3 (1), 50 (2013). (in Russian) Crossref
8. R.L. Athey, J.B. Moore. Progress Report on the Gatorizing™ Forging Process, SAE Technical Paper. 751047 (1975). Crossref
9. E. Ghassemali. Encyclopedia of Materials: Metals and Alloys. 4, 129 (2022). Crossref
10. A. Chamanfar, H.S. Valberg, B. Templin, J.E. Plumeri, W.Z. Misiolek. Materialia. 6, 100319 (2019). Crossref
11. S.S. Satheesh Kumar, T. Raghu, P.P. Bhattacharjee, G. Appa Rao, U. Borah. Materials Characterization. 146, 217 (2018). Crossref
12. E. Akca, A. Gursel. Periodicals of engineering and natural sciences. 3 (1), 15 (2015). Crossref
13. F.Z. Utyashev, O.A. Kaybyshev, V.A. Valitov. Method for manufacturing axially symmetrical parts and blank making process for performing the same. Patent RU No 2119842, 10.10.1998. (in Russian)
14. F.Z. Utyashev, O.A. Kaibyshev, V.A. Valitov. Method For Processing Billets From Multiphase Alloys. European Patent No EP 0909339 B1, 21.11.2001.
15. O.A. Kaibyshev, G.A. Salishchev, R.M. Galeev, R.Ya. Lutfullin, O.R. Valiakhmetov. Processing method for titanium alloys. RF patent No 2134308, 10.08.1999. (in Russian)
16. R.R. Mulyukov. Rossiyskiye nanotekhnologii. 2 (7-8), 38 (2007). (in Russian)
17. A.A. Ganeev, V.A. Valitov, M.I. Nagimov, V.M. Imayev. Letters on Materials. 10 (1), 100 (2020). (in Russian) Crossref
18. V.A. Valitov. Formation of Nanocrystalline Structure Upon Severe Thermomechanical Processing and its Effect on the Superplastic Properties of Nickel Base Alloys. In: 8th International Symposium on Superalloy 718 and Derivatives (ed. by E. Ott, A. Banik, J. Andersson, I. Dempster, T. Gabb, J. Groh, K. Heck, R. Helmink, X. Liu, A. Wusatowska-Sarnek). The Minerals, Metals & Materials Society (2014) pp. 739 – 750. Crossref
19. Yu.A. Pestov, V.N. Semenov, V.I. Novikov, B.A. Kozykov, K.I. Nedashkovsky, E.A. Kukin, G.G. Derkach, Yu.V. Movchan, B.I. Katorgin, V.K. Chvanov, S.S. Golovchenko, N.A. Sorokina, V.P. Stepanov, L.S. Bulavina, Yu.I. Rusinovich, I.A. Rastorgueva, V.P. Ponomareva. Precipitation hardening weldable nickel-based alloy. RF patent No 99111620, 27.04.2001. (in Russian)
20. A.P. Shlyamnev. Corrosion-resistant, heat-resistant and high-strength steels and alloys: a Handbook. Moscow, Prommet-splav (2008) 336 p. (in Russian)
21. J. Huang, G. Xu, H. Qin, L. Zheng. Scanning. 2020 (5), 1 (2020). Crossref
22. M. Pérez, Ch. Dumont, O. Nodin, S. Nouveau. Materials Characterization. 146, 169 (2018). Crossref
23. N.V. Lopatin, S.N. Gorbushina, I.P. Semenova, G.S. Dyakonov, E.A. Kudryavtsev, S.V. Vydumkina. Computer research and modeling. 6 (6S), 975 (2014). (in Russian) Crossref
24. I.A. Burlakov, V.A. Valitov, A.A. Ganeev, et. al. Journal of Machinery Manufacture and Reliability. 45 (5), 469 (2016). Crossref
25. E.V. Galieva. Solid-phase joining of an intermetallic alloy based on Ni_3Al and a heat-resistant nickel superalloy using superplastic deformation: PhD thesis. IMSP RAS, R.F. (2021) 195 p.
26. E.V. Galieva, V.A. Valitov, E.Yu. Klassman. Fundamental problems of modern materials science. 17 (4), 461 (2020). (in Russian) Crossref
27. V.A. Valitov, R.R. Mulyukov, M.F. X. Gigliotti, P.R. Subramanian. In: Superalloys 2008 (ed. by R.C. Reed, K. A. Green, P. Caron, T. P. Gabb, M. G. Fahrmann, E. S. Huron, S. A. Woodard). TMS (2008) pp. 325-331. Crossref
28. V.A. Valitov, Sh.Kh. Mukhtarov, Yu.A. Raskulova. The Physics of Metals and Metallography. 102 (1), 97 (2006). Crossref
29. V.A. Valitov. Issues of materials science. 52 (4), 311 (2007). (in Russian)